Cancer Research

Macrophage Expression of Hypoxia-Inducible Factor-1α Suppresses T-Cell Function and Promotes Tumor Progression

Introduction

T cells can have potent effects on tumor progression (1, 2); however, it is evident that many solid tumors are resistant to immune responses and immune cell attack. Although much effort has been devoted to increasing immune responses against tumors, this is hampered by localized immunosuppression of the adaptive immune system (3, 4).

The tumor microenvironment differs from that of normal tissues in several respects. Tumors are frequently marked by regions of hypoxia, as rapidly dividing malignant cells outpace the capacity of the established vasculature to deliver oxygen and nutrients (5, 6). Hypoxia-inducible factor-1α (HIF-1α) is a constitutively expressed bHLH transcription factor expressed in nearly all mammalian cell types, including macrophages and neutrophils (7). Tissue-specific genetic deletion of HIF-1α largely ablates the cellular transcriptional response to decreasing oxygen tension in macrophages (8, 9). Initial characterization of the role of HIF-1α in myeloid cells showed that it was essential for the capacity to mount a full immune response, suggesting a mechanism to amplify innate immune responses under low oxygen tensions—conditions typically found in wounds or infected tissues (8, 10). Several studies have shown the immunosuppressive nature of macrophages and myeloid-derived suppressor cells (MDSC) in tumor-bearing hosts (11–15). Hypoxia is a hallmark of neoplastic growth; however, it is unclear how cellular hypoxic response, mediated at the transcriptional level by HIF-1α, acts on the suppressive capacity of tumor-infiltrating myeloid cells.

Two L-arginine–consuming enzymes have been implicated in myeloid T-cell suppression: the inducible nitric oxide synthase (iNOS/NOS2, NM010927) and arginase I (ArgI, NM007482). Activation of myeloid iNOS acts to suppress T cells by production of nitric oxide, which then inhibits signal transduction (16, 17). Other groups have also documented the role of ArgI-mediated L-arginine depletion in T-cell suppression (13, 18). Myeloid cells are capable of a striking increase in iNOS and ArgI enzyme levels following specific signaling events, and this increase is further potentiated by low oxygen tensions found in tumors, suggesting a role for HIF-1α–dependent hypoxic regulation of iNOS and ArgI in myeloid cell–mediated T-cell suppression (9).

Materials and Methods

Cell culture, cell lines, and hypoxic incubation

Resident peritoneal macrophages were obtained through peritoneal lavage with 10 mL of cold PBS without Ca^{2+}/Mg^{2+}. Resulting cells were pelleted, and RBCs were lysed with ACK buffer, resuspended in RPMI 1640/10% fetal bovine serum (FBS)/1% penicillin-streptomycin, and plated on 15-cm Petri dishes overnight. Medium was then aspirated and plates were washed with Dulbecco's PBS two times before addition of cold PBS + 15 mmol/L EDTA. After incubation for 10 to 15 minutes, adherent cells were removed by pipet-ting, which removed the majority of the cells followed by light scraping to maximize yield. Bone marrow–derived macrophages (BMDM) were obtained by incubating the lavage of femur and tibia from rodents of the indicated genotype with RPMI 1640/20% FBS/30% L929 cell supernatant/1% penicillin-streptomycin/1% amphotericin B in two 15-cm Petri dishes. After 6 days in culture, medium was aspirated and the dish was washed once in PBS before harvesting in the same manner as resident peritoneal macrophages detailed above. For gene expression or Western blot analysis, cells were then plated in RPMI 1640 overnight before experimental manipulation. Hypoxic incubation was performed in a water-jacketed, humidified, multigas tissue culture incubator equipped with nitrogen and carbon dioxide, which flushes out oxygen until reaching a final concentration of 1% oxygen/5% carbon dioxide. Parallel normoxic incubation was carried out in standard humidified 5% carbon dioxide tissue culture incubators. Coculture experiments were performed in 0.4-μm-pore Transwell plates (Corning Life Sciences) in either 6- or 24-well formats following the manufacturer's instructions. Polyoma middle T (PyMT) mammary epithelial cells (MEC) were isolated from endpoint animals by growing out adherent epithelial cells after collagenase digestion of PyMT tumors, and thus are polyclonal with a homogeneous, adherent, epithelioid appearance.

T-cell macrophage coculture proliferation assay

Resident peritoneal macrophages or BMDMs were isolated from *HIF-1α* wild-type (WT) or HIF DF/LysM-cre$^+$ (DF= double floxed, i.e., homozygous for the conditional allele) littermates as described above. Splenocytes were isolated from a separate WT C57BL/6J mouse by removal of the spleen, gentle squeezing between frosted glass slides, and brief ACK hypotonic RBC lysis. T cells were purified using the CD4$^+$ T Cell Isolation kit from Miltenyi Biotec, which uses negative selection. The resulting purified T-cell suspension lacking platelets and RBCs was labeled with carboxyfluorescein diacetate succinimidyl ester (CFSE; Invitrogen) to later quantify T-cell proliferation. CFSE-labeled T cells (1×10^5) were plated in 24-well CD3$^+$ antibody–coated (5 μg/mL) plates with CD28-soluble antibody (1 μg/mL) added to the medium to induce T-cell proliferation either with or without indicated ratios of macrophages, which were added 3 hours after T-cell activation [protocol modified from Atochina and colleagues (19)]. Cells were then incubated in normoxia or hypoxia (1% oxygen) for 60 hours with or without the iNOS-specific inhibitor 1400W at 100 μmol/L. Analysis of cells was performed on a FACSCalibur flow cytometer after labeling with fluorescent antibodies and propidium iodide to exclude dead cells.

PyMT model of carcinogenesis in backcrossed C57BL/6J/HIF-1α$^{+f/+f}$ murine hosts

Backcrossed mice carrying the PyMT oncogene under the control of the murine mammary tumor virus (MMTV) long terminal repeat (20), here referred to simply as PyMT, were obtained from the lab of Dr. Leslie Ellies (University of California at San Diego Medical Center, La Jolla, CA). Individual transgenic alleles for LysM-cre (21) and HIF-1α flox (22) were backcrossed to C57BL/6J to >99% using speed backcrossing single-nucleotide polymorphism genotyping service (The Jackson Laboratory). After one further cross to C57BL/6J, mice were crossed to obtain female HIF-1α$^{+f/+f}$/PyMT$^{+/-}$/LysM-cre$^{+/-}$ (experimental) and female littermate control *HIF-1α*$^{+f/+f}$/PyMT$^{+/-}$/LysM-cre$^{-/-}$. LysM-cre efficiently excises floxed sequences in neutrophils and macrophages, but not CD11c$^+$ dendritic cells (8, 21). We observed abundant macrophage infiltration but little to no neutrophil infiltration of tumors (data not shown). We use the terms "myeloid" or "macrophage deletion" in this work to refer to the pattern of deletion generated by LysM-cre.

Enzyme assays

Tumors were rapidly dissected out of endpoint hosts and flash frozen in liquid N_2. After polytron homogenization of the sample on ice and pelleting of insoluble material, arginase activity from the same samples was determined by quantifying the abundance of urea after lysate incubation with an excess of L-arginine, as shown by other groups (23). Arginase activity was then normalized to total protein in the lysate as measured by the bicinchoninic acid assay (Thermo Fisher Scientific/Pierce).

Flow cytometry, histology, immunohistochemistry, antibodies, recombinant cytokines, and real-time PCR reagents

Single-cell suspensions of tumors were generated by chopping with a razor blade followed by incubation at 300 rpm at 37°C for 60 minutes in 5 mL of 0.22-μm filtered RPMI 1640 (no serum)/0.05% to 0.1% collagenase A (Roche Diagnostics). RPMI 1640/10% FBS/25 mmol/L HEPES/1% penicillin/streptomycin was used for all experiments, except where T cells were cultured, where 55 μmol/L β-mercaptoethanol (Invitrogen) was added as is standard in murine T-cell culture.

All fluorescent antibodies, recombinant mouse IFNγ, and interleukin (IL)-4 were from eBioscience, with the exception of F4/80 (AbD Serotec). ABC Elite HRP or AP kits from Vector Labs were used for immunohistochemistry following the manufacturer's instructions. Biotin anti-CD31 and biotin anti–proliferating cell nuclear antigen (PCNA) were from BD Pharmingen. Rabbit anti-ArgI was from Santa Cruz Biotechnology. Rabbit anti-iNOS was from Calbiochem/EMD

Published OnlineFirst September 14, 2010; DOI:10.1158/0008-5472.CAN-10-1439

Biosciences. Colorimetric terminal deoxynucleotidyl transferase–mediated dUTP nick end labeling (TUNEL) staining was performed using the Promega DEADend kit.

Gene expression was carried out on an ABI 7700 normalized to levels of 18S rRNA. Target and reference real-time reactions were run in duplicate, and the average was used to calculate $\Delta\Delta C_T$. Error bars indicate the SEM of multiple samples.

Measurement of IFNγ production by tumor-infiltrating lymphocytes

Single-cell suspensions of PyMT tumors from myeloid HIF WT or knockout (KO) tumors were added to anti-CD3 antibody–coated plates. BD Biosciences GolgiStop and CD28 antibody were added to the medium, and 8 hours later, cells were stained for CD4/CD8 on the surface and then intracellularly with anti-IFNγ PE using the Cytofix/Cytoperm kit from BD Biosciences before flow cytometry as described above.

Results

Creation of myeloid HIF-1α–null mammary tumor transgenics

To gain insight into the role of the myeloid hypoxic response in the tumor microenvironment, we used a well-characterized mouse strain that allows the study of tumor progression, the MMTV long terminal repeat promoter driving the PyMT oncogene specifically in mammary tissue: the MMTV-PyMT model (20, 24). As part of our initial characterization of HIF-1α$^{+f/+f}$/PyMT$^{+/-}$/LysM-cre$^{+/-}$ mice, we determined that mammary gland development was normal in mice lacking HIF-1α. There were no differences in epithelial ductal tree formation detected between the genotypes; both displayed branching structures that extended through the entire fat pad—evidence of normal mammary gland development (data not shown). After tumor growth, initial immunohistochemical staining of myeloid WT mice revealed a prominent tumor macrophage F4/80$^+$ infiltrate, consistent with reports by others (data not shown; ref. 25).

We found that there is efficient deletion of HIF-1α in myeloid cells found in tumor-bearing mice, including Gr1$^+$CD11b$^+$ MDSCs (Supplementary Fig. S1; refs. 8, 21). We also detected tumor infiltration with CD8$^+$ T cells (data not shown). The PyMT model exhibits several important characteristics consistent with clinically relevant tumor scenarios, including stage-wise histologic progression, marked macrophage infiltration, and a spontaneous endogenous T-cell response, which is eventually suppressed during tumor growth (24, 26). To investigate the role of myeloid HIF-1α in this

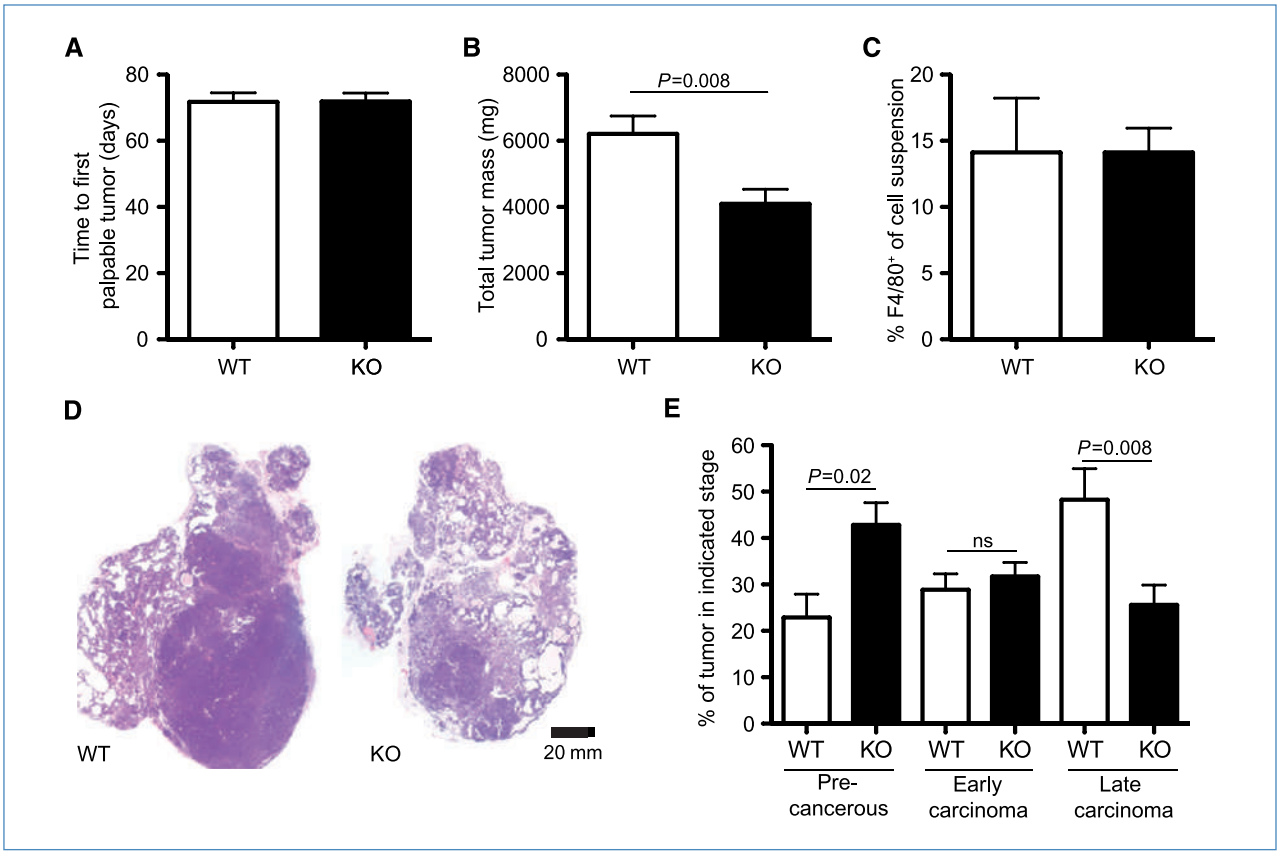

Figure 1. Deletion of HIF-1α in macrophages results in lower endpoint tumor mass despite equivalent latency and macrophage infiltration. (A) Latency or time to first tumor, (B) total mass of all tumors at 20-wk endpoint (n = 8). C, percentage of F4/80$^+$ macrophages in single-cell suspensions generated from tumors (n = 4). D, macroscopic H&E staining of typical tumors. E, histologic stage analysis of tumors. Columns, mean; bars, SE.

Published OnlineFirst September 14, 2010; DOI:10.1158/0008-5472.CAN-10-1439

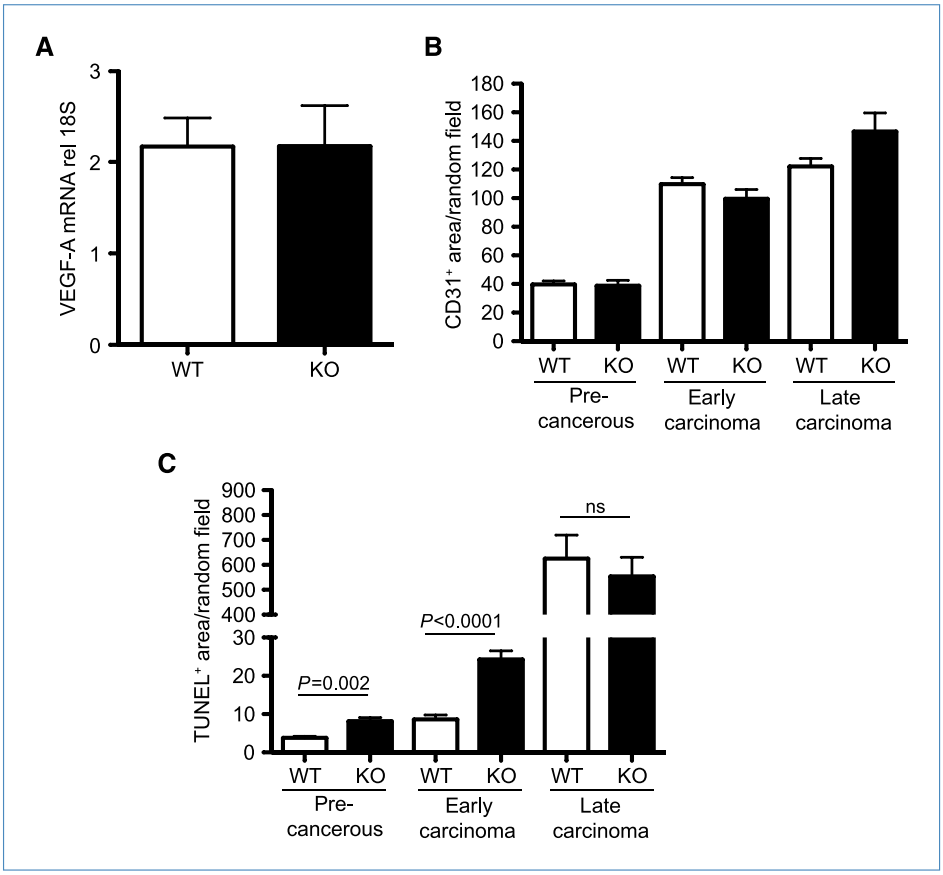

Figure 2. Myeloid HIF-1α–null tumors have similar VEGF-A mRNA levels and similar stage-specific microvascular densities but different levels of cell death. A, VEGF-A mRNA from whole tumor lysates relative to 18S rRNA (n = 8). B, stage-specific quantitation of CD31 staining of random fields (n = 8). C, stage-specific quantitation of TUNEL positivity of random fields (n = 8). Columns, mean; bars, SE.

relevant setting, we designed a breeding strategy that would yield backcrossed, myeloid cell–specific KOs of HIF-1α in the PyMT model of mammary carcinogenesis.

Myeloid deletion of HIF-1α results in reduced tumor mass and retarded tumor progression

One important control for early tumor-promoting events as well as for the efficacy of inbred strain backcrossing is latency or time to the first detectable tumor growth; we found no difference in latency between genotypes (Fig. 1A). In this model, 2 to 3 months pass from detection of first tumor growth by palpation to experimental endpoint; during this time, tumors undergo growth and stage-wise histologic progression. Myeloid deletion of HIF-1α resulted in a marked decrease in endpoint tumor mass (Fig. 1B), despite similar levels of tumor infiltration with F4/80$^+$ macrophages (Fig. 1C). Remarkably, histologic analysis revealed striking differences between the tumors, with HIF-1α myeloid–null tumors having a more nodular and cell-dense appearance. Analysis by immunohistochemistry for PCNA, a marker for cell proliferation, showed extensive dividing cell populations in the advanced histologic stage/dense cell masses, which were more abundant in the WT control animals (data not shown). The PyMT model has been characterized with regard to human equivalents of tumor stages/progression (24). We used this stage classification technique to grade tumors into three levels of histologic progression by quantifying the area occupied by each stage from midline cross-sections of the transformed glands. The progression follows from what we refer to as a "precancerous stage," hyperplasia and adenoma/MIN premalignant lesions, which still retain some normal ductal and acinar mammary gland morphology; to a more epithelial cell–dense early carcinoma with some stromal invasion; and finally an invasive, high mitotic index, late-stage carcinoma. As reported by careful work from Lin, Pollard, and colleagues, similar human equivalents of these stages were florid ductal hyperplasia, ductal carcinoma *in situ* with early stromal invasion, and poorly differentiated invasive ductal carcinoma, respectively. In our study, this histologic stage analysis revealed that tumors from WT mice were more advanced, with increased amounts of late carcinoma tumor mass. Mice lacking myeloid cell HIF-1α had significant increases in precancerous stages relative to WT animals (Fig. 1D and E), indicating that there is a delay in histologic progression of tumors in the mutant mice.

Loss of HIF-1α does not affect vascular endothelial growth factor-A levels or vascularization of mammary tumors

HIF-1α regulates the angiogenic factor vascular endothelial growth factor-A (VEGF-A; refs. 22, 26, 27). Although VEGF-A is

Published OnlineFirst September 14, 2010; DOI:10.1158/0008-5472.CAN-10-1439

expressed by tumor-associated macrophages (28), whole tumor lysate VEGF-A levels were nearly identical in WT and myeloid HIF-1α–null tumors (Fig. 2A). $CD31^+$ staining of tumor sections to determine stage-dependent vascular density revealed no significant changes in a stage-specific analysis (Fig. 2B); thus, loss of HIF-1α does not result in an altered level of tumor vascularization. We have previously shown that mice lacking myeloid cell VEGF-A expression have increased tumor mass and progression (28); this is a further argument against VEGF-A expression as a determinant of the phenotype described here.

Increased tumor apoptosis following loss of myeloid HIF-1α

Staining for cell death and apoptosis by TUNEL revealed that there was a highly significant increase in cell death in the myeloid HIF-1α–null mice at early and middle stages of tumor progression (Fig. 2C). This indicated that loss of HIF-1α in the myeloid lineage was causing an increase in tumor cell death; this would act to slow the progression of the tumors and reduce their mass. Because angiogenesis did not seem to be affecting tumor growth, and T-cell cytotoxicity can result in TUNEL positivity, we set out to test how T-cell function was affected by macrophages and hypoxia.

Macrophages inhibit T-cell proliferation under hypoxia

T-cell activation and proliferation are essential steps in the adaptive immune response, and increase the clonal frequency of antigen-specific T cells, as well as in inducing differentiation into effector and memory cells. Subsequent activation of effector or memory cells results in cytokine release and antigen-specific cytotoxicity. Given the infiltration of the experimental mammary tumors with macrophages and T cells, we tested the capacity of T cells cocultured with macrophages to proliferate under normoxia and hypoxia. In this assay, T-cell division can be detected by flow cytometry. Notably, only the higher ratios of macrophages inhibited T-cell proliferation under normoxia (Fig. 3A–C). Careful titration of macrophage/T-cell ratios, however, revealed that reduced oxygen levels augmented T-cell inhibition of macrophages. T cells are able to proliferate under hypoxia (1% oxygen) after CD3/CD28 stimulation (1:80 condition; Fig. 3B). However, when macrophages were 5% of the total cell number, cell cycle progression was markedly blocked (1:20 conditions; Fig. 3A–C), whereas normoxic proliferation at this ratio was largely unaffected. Figure 3C quantitates this hypoxic potentiation of suppressive capacity over a range of macrophage/T-cell ratios and shows that lowering oxygen tension increases macrophage inhibition of T-cell proliferation and viability.

Macrophage T-cell suppression in hypoxia is HIF-1α/iNOS dependent

To test the role of HIF-1α in macrophage-mediated hypoxic T-cell suppression, we carried out cocultures with macrophages derived from *HIF-1α*$^{+f/+f}$/LysM-cre$^{+/-}$ (macrophage HIF KO) bone marrow (Fig. 4). In Fig. 4A, we show that under normoxia, no change in suppressive capacity between the

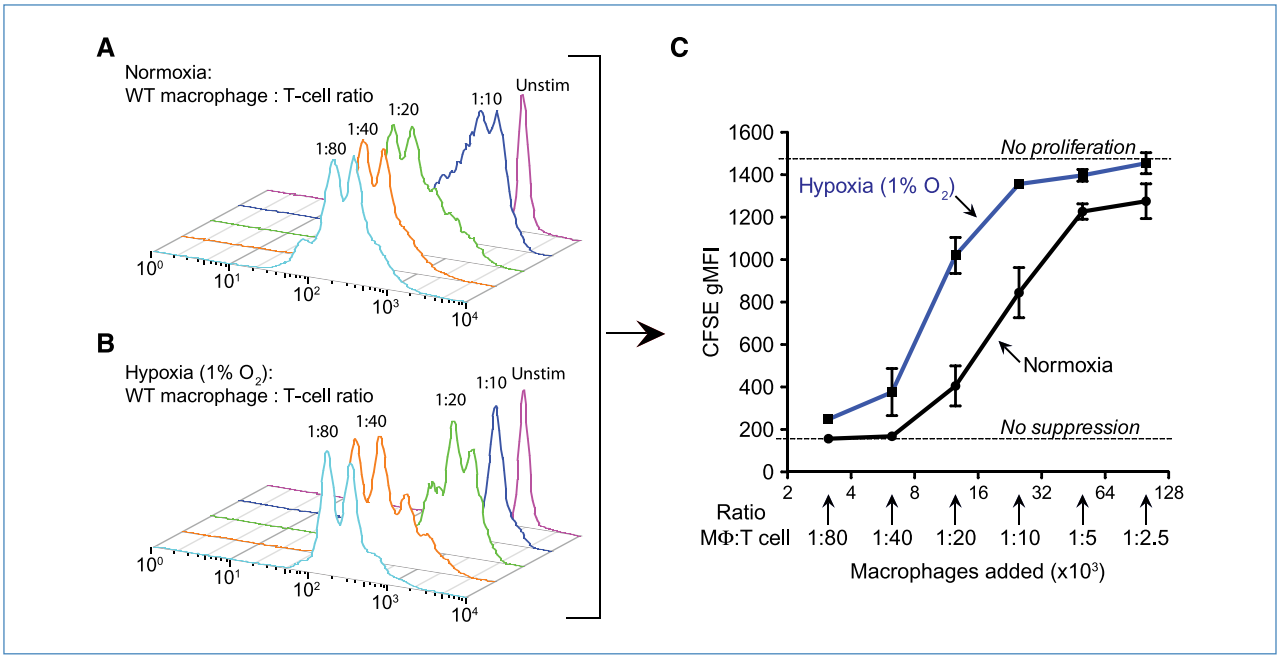

Figure 3. Macrophage suppression of T-cell proliferation is augmented under hypoxia. A and B, representative quantitation of T-cell proliferation as measured by dilution of CFSE. Purified T cells were loaded with CFSE, activated *in vitro* by CD3/CD28 and cocultured with the indicated ratio of BMDMs for 60 h under (A) normoxia or (B) 1% oxygen (hypoxia). C, an independent replicate experiment graphically depicting hypoxia-potentiated macrophage suppression of T-cell proliferation ($n = 2$). The increased hypoxia/macrophage-dependent suppression was observed in eight independent experiments with various macrophage populations including resident peritoneal macrophages (three times), thioglycollate-elicited macrophages (two times), and BMDMs (three times). Columns, mean; bars, SE.

Published OnlineFirst September 14, 2010; DOI:10.1158/0008-5472.CAN-10-1439

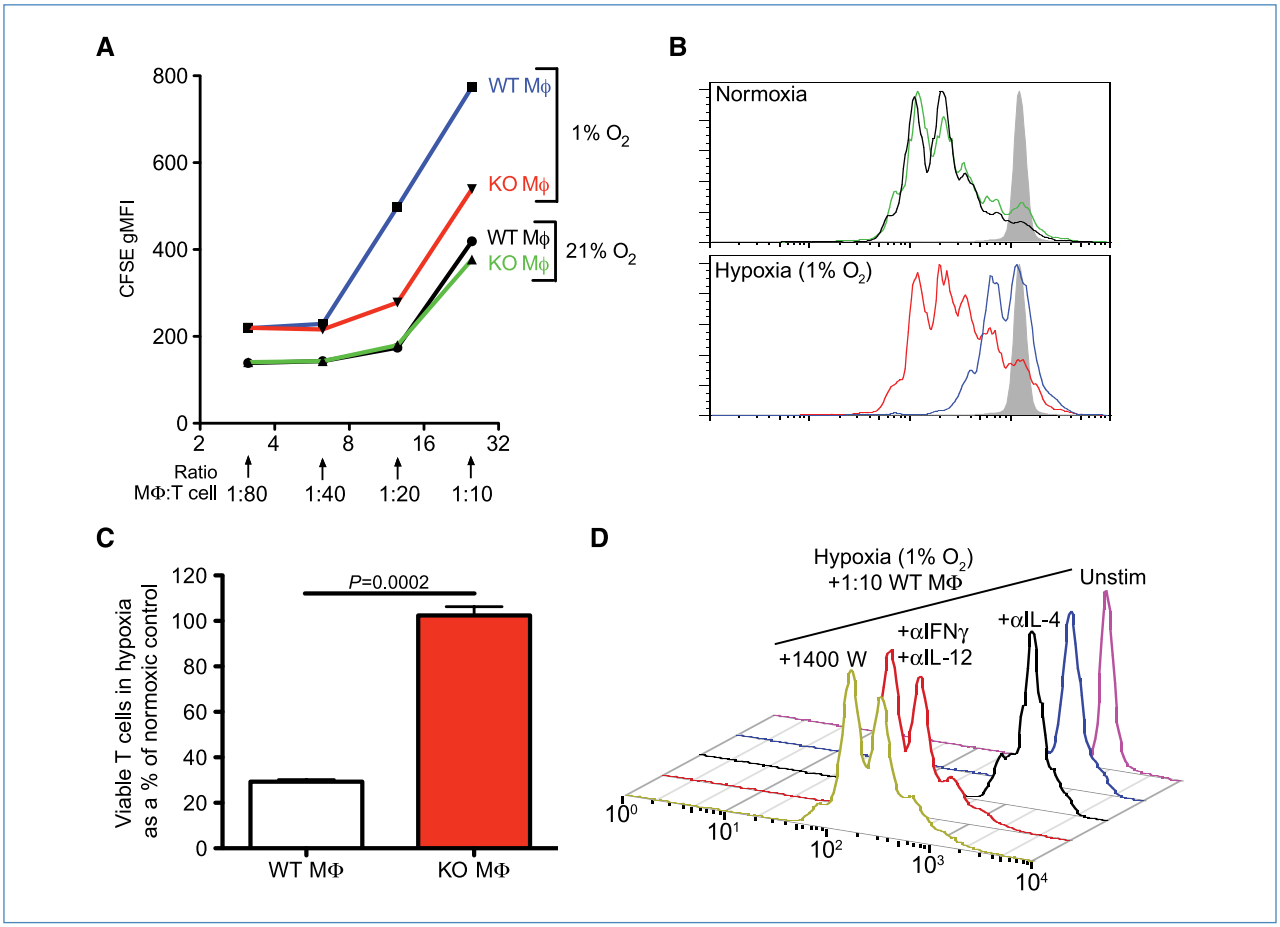

Figure 4. HIF-1α–null macrophages fail to augment T-cell suppression under hypoxia, and WT-suppressive effect is dependent on HIF-1α upregulation of macrophage iNOS and can be blocked by neutralizing classic proinflammatory cytokines or specific iNOS inhibition. A, CFSE dilution after 60-h T-cell activation in normoxia or 1% oxygen with the indicated number of macrophages (Mφ) (in thousands) added to the cultures. B, representative overlays of CFSE dilution in T cells after activation and coculture at 1:20 macrophage/T-cell as in A. Samples are from an independent experiment yet can be identified by the same color scheme as in A. Control unstimulated CFSE-loaded T cells appear in gray. C, viable T cells recovered in hypoxic conditions as a percentage of the amount recovered in normoxic conditions at 1:20 macrophage/T cells (n = 2). All results are representative of three independent experiments. D, representative CFSE dilution of purified T cells after activation and coculture for 60 h with WT BMDMs with the cytokine-neutralizing antibodies (α to indicate antibody) or the iNOS inhibitor 1400W added as indicated. Similar results were observed in three independent experiments.

genotypes exists over a wide range of macrophage/T-cell ratios (green and black lines). In hypoxia, however, HIF-1α–null macrophages were poor inhibitors of T-cell proliferation at 1:20 and higher ratios, ratios where WT macrophages induced a potent cell cycle arrest [Fig. 4A (red and blue lines) and B (CFSE traces)]. Using propidium iodide exclusion to count viable cells collected during a fixed time and flow rate, we show in Fig. 4C that T cells incubated with WT macrophages at 1:20 have only 30% of the viability of those incubated with an equal number of HIF-1α–null macrophages. These results show that macrophage-mediated suppression of T-cell proliferation in hypoxia is HIF-1α dependent.

Activated T cells rapidly produce Th1 and Th2 cytokines (e.g., IFNγ and IL-4) following stimulation. Macrophages have a specific and inverse transcriptional response to these cytokines, increasing iNOS and downregulating ArgI expression after IFNγ stimulation, for example, while increasing ArgI and downregulating iNOS expression after IL-4 stimulation (29); both of these occur in a HIF-dependent fashion when macrophages are hypoxic (9). Although both iNOS and ArgI have been extensively reported to suppress T-cell function (30), iNOS can act acutely to block T-cell proliferation by nitric oxide and subsequent peroxynitrite formation, whereas ArgI creates immunosuppressive microenvironments by depleting local L-arginine first—an indirect effect unlikely to affect T-cell proliferation in an acute *in vitro* assay (31). Because activated T cells make a mixture of Th1 and Th2 cytokines, neutralizing antibodies to IFNγ and IL-12 can generate a Th2-type cytokine profile (by leaving IL-4 as the dominant T-cell–derived cytokine), whereas neutralizing antibodies to IL-4 generate a Th1 profile.

To first test the role of the HIF target and Th1-induced gene iNOS in suppression, we blocked its activity with the chemical compound 1400W, an iNOS-specific inhibitor (32). These experimental conditions are reported in Fig. 4D; as can be seen, WT macrophages at a 1:10 ratio with T cells arrest T-cell

Published OnlineFirst September 14, 2010; DOI:10.1158/0008-5472.CAN-10-1439

proliferation under hypoxia (blue trace), leaving them at proliferation rates comparable with unstimulated cells (purple trace). The addition of neutralizing antibodies to IL-4 fails to rescue T-cell proliferation. However, addition of neutralizing antibodies to IFNγ and IL-12 releases the T cells from the macrophage/hypoxia-potentiated cell cycle progression arrest. Considering the data discussed above, a suppressive effect that depends on HIF-1α, hypoxia, and IFNγ, yet can be rescued with IL-4, would suggest an iNOS-dependent suppression. Indeed, treatment of a 1:10 macrophage/T-cell culture with 1400W fully restores the capacity for robust T-cell proliferation under hypoxia (Fig. 4D, yellow trace, +1400W). Macrophages derived from iNOS$^{-/-}$ mice were similarly unable to inhibit T-cell proliferation in this acute assay (data not shown). It should be noted that T cells and other immune cells engaged in cytotoxic action against tumors typically produce IFNγ.

PyMT tumor-infiltrating macrophages have a mixed M1/M2 polarization signature independent of HIF-1α

We next wished to determine if HIF-1α had any affect on polarization of macrophages and to characterize the polarization state of tumor-infiltrating macrophages in the MMTV-driven mammary tumors (i.e., determine whether they were classically or alternatively activated; refs. 33, 34). To accomplish this, BMDMs were treated with classic M1 (IFNγ) or alternatively activating M2 (IL-4) cytokines and cell surface expression of markers reported to be upregulated by an M1/classic polarization state were measured (MHC II and CD86). No difference was found in the capacity of HIF-1α WT or nullizygous macrophages to polarize under IFNγ-, IL-4–, and IL-10–stimulated conditions under hypoxia, as determined by multiple cell surface markers correlated with activation state. However, macrophages infiltrating tumors displayed a mixed activation phenotype, displaying properties of both classically activated and alternatively activated macrophages (Supplementary Fig. S2).

Macrophage HIF-1α–dependent induction of ArgI after coculture with PyMT MECs under hypoxia

To determine whether cancer cells combined with hypoxia might induce the iNOS or ArgI genes in macrophages in close proximity, we carried out coculture studies using Transwell tissue culture plates. BMDMs were added to the bottom of a Transwell dish, and a PyMT MEC line derived from a WT tumor (data not shown) was plated in the upper well. In this culture design, both cells share the same medium via a porous membrane (Fig. 5A, left). The pores allow diffusion of soluble factors, but not of cells. We tested HIF-1α–null macrophages in normoxia or hypoxia in the presence or absence of MEC for 24 hours. Subsequent Western blotting revealed that ArgI is markedly induced in macrophages by coculture with MEC (Fig. 5A, right). However, ArgI was abundant only under hypoxia and was dependent on HIF-1α (Fig. 5A, right). In

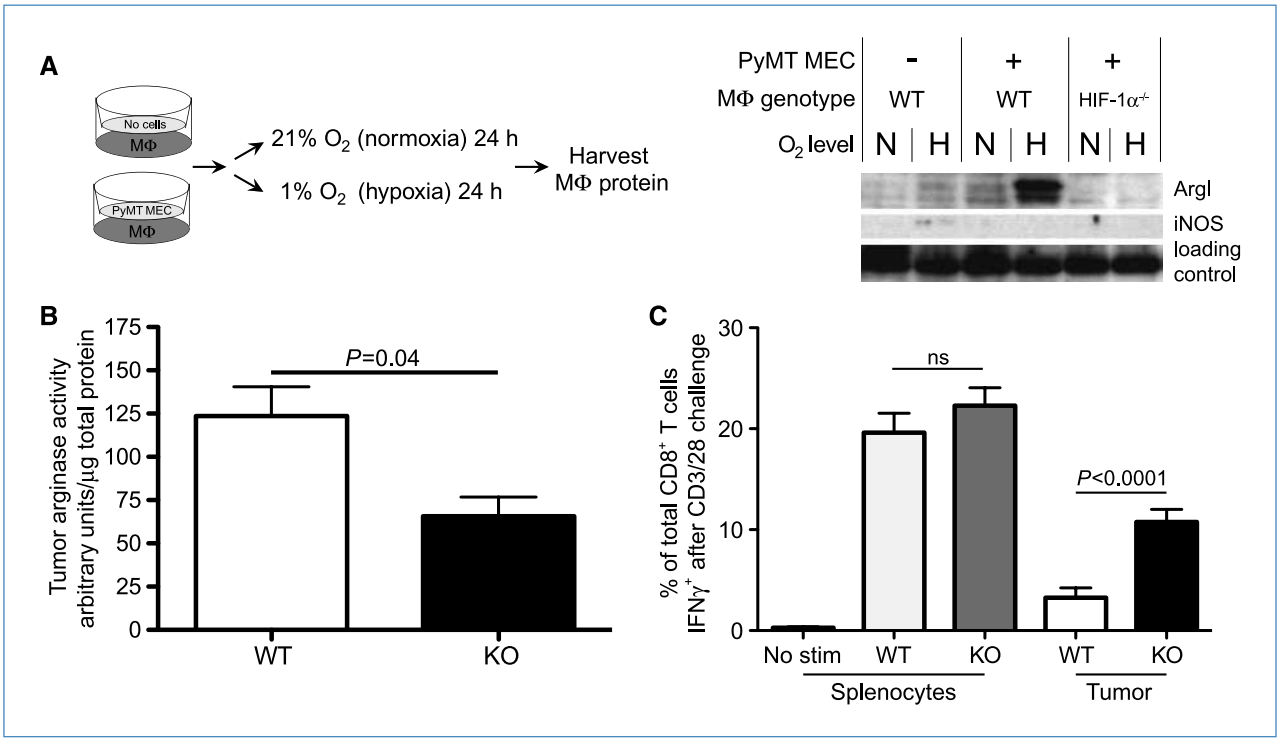

Figure 5. HIF-1α–dependent ArgI induction by tumor cells and hypoxia is associated with tumor T-cell suppression. A, *in vitro* coculture of macrophages with or without a PyMT MEC line in normoxia or hypoxia for 24 h. Left, experimental design; right, protein analysis/detection by Western blot. B, arginase enzyme activity quantitation of myeloid HIF-1α WT PyMT tumor lysates (n = 9). C, single-cell suspensions of spleens or PyMT tumors WT or KO for myeloid HIF-1α were stimulated *in vitro* with CD3/CD28 and the percentage of T cells making IFNγ after 8 h is reported (n = 12). Columns, mean; bars, SE.

Published OnlineFirst September 14, 2010; DOI:10.1158/0008-5472.CAN-10-1439

contrast, iNOS showed a modest induction only in hypoxia without MEC at the limit of detection. This shows that under hypoxia, tumor cells are capable of releasing soluble factor(s) that potently activates the ArgI-dependent arm of the immunosuppressive repertoire of macrophages.

Macrophage HIF-1α acts to suppress cytotoxic T-cell responsiveness within tumors

HIF-1α–regulated enzymes ArgI and iNOS can induce immunosuppression in T cells (18, 35–37). We performed enzyme activity assays on whole PyMT tumor lysates from myeloid HIF-1α WT or nullizygous mice. ArgI activity was significantly higher in lysates from WT mice, as expected (Fig. 5B). iNOS activity in WT tumors was higher and with a larger variance, but the difference was not statistically significant (data not shown). These data seem to mirror the PyMT/macrophage coculture (Fig. 5A), which was more effective at inducing ArgI than iNOS. In our analysis of single-cell suspensions from tumors, we found no significant difference in the number of infiltrating $CD8^+$ T cells (data not shown). Given the high amount of immunosuppressive ArgI activity in WT tumors, it was important to test the responsiveness of T cells taken directly from WT and myeloid HIF-1α–null host tumors. One key measurement of T-cell responsiveness is the ability to produce IFNγ immediately following stimulation. IFNγ production after activation *in vitro* has been reported to correlate well with T-cell antitumor cytotoxic potential and is a key measure of T-cell effector capacity (38–40). To test tumor T-cell responsiveness from myeloid HIF-1α WT and null tumors, the fraction of T cells that make IFNγ after a strong, pan–T-cell stimulation with anti-CD3/CD28 antibody of tumor single-cell suspensions was carried out. There was a marked and highly significant increase in the fraction of T cells producing IFNγ from myeloid HIF-1α–null tumors when compared with T cells from WT tumors (Fig. 5C). This shows that HIF-1α expression in myeloid cells is correlated with suppression of tumor cytotoxic T cells.